Prediction of anchorage performance of headed bars using artificial neural networks

*Jang-Woon Baek[1] , Beom-Jung Kim[2], and Hyeon-Jong Hwang[3]

[1], [2] Department of Architectural Engineering, Kyung Hee Univ., Yongin-si, 17104, Korea*
[3] School of Architecture, Konkuk Univ., Seoul, 05029, Korea
[1] baekjw@khu.ac.kr

ABSTRACT

Recently, machine learning has been widely used in civil engineering, particularly to accurately predict design strengths of structural members, because better design can be achieved using the advanced computer intelligence and test results. The anchorage capacity of headed bars shows large variations according to design conditions, such as diameter of reinforcing bars, location of anchorage, and the use of fiber-reinforced concrete. In the present study, to more accurately predict the bond performance of headed bars, an artificial neural network model (ANN) was presented using 270 existing experimental studies for beam-column joint test. Comparisons showed that the ANN model improved the accuracy of the design methods. A parametric study to investigate the effects of each design variable used in the ANN model, and simplification for the ANN model are required to be used in practice.

1. INTRODUCTION

Since development lengths of headed bars are generally shorter than those of straight bars or hooked bars, for better constructability and cost saving, headed bars are widely used under various conditions, including ends of flexural members, compression-compression-tension (CCT) node, lap splice, beam-column joint, and transverse reinforcement. Particularly, the use of the headed bars is preferred in beam-column joints and structures with large-diameter bars such as nuclear power plants to reduce reinforcing bar congestion and consequently to decrease the required development length. Further, in place of the straight bars or hooked bars, the headed bars have recently been applied to new materials such as fiber-reinforced concrete,

---

[1] Assistant Professor
[2] Student
[3] Associate Professor

ultra-high-performance concrete (UHPC), high-strength reinforcing bars, and large-diameter bars.

Current design codes specify headed bar development lengths including ACI 318-19 (ACI Committee 318, 2019) and Model Code 2010 (International Federation for Structural Concrete (fib), 2013). To evaluate the anchorage strength of headed bars under various design conditions, CCT node test, beam end test, splice test, and beam-column joint test should be performed as shown in **Fig. 1**. However, the number of test results for headed bars is currently limited. For this reason, current design codes define the design equation for headed bar development length based on that of hooked bars with relatively limited applications. Further, current design codes limit the application range of the design equations, considering the material properties, minimum concrete cover, head size, and spacing of headed bars. Thus, to use headed bars in various design conditions, the development length of headed bars needs to be accurately evaluated and a large number of test results are required to verify the effect of new design parameters. To achieve more accurate and economical design, significant efforts have been made.

(a) CCT node test   (b) Beam end test   (c) Splice test   (d) Beam-column joint test
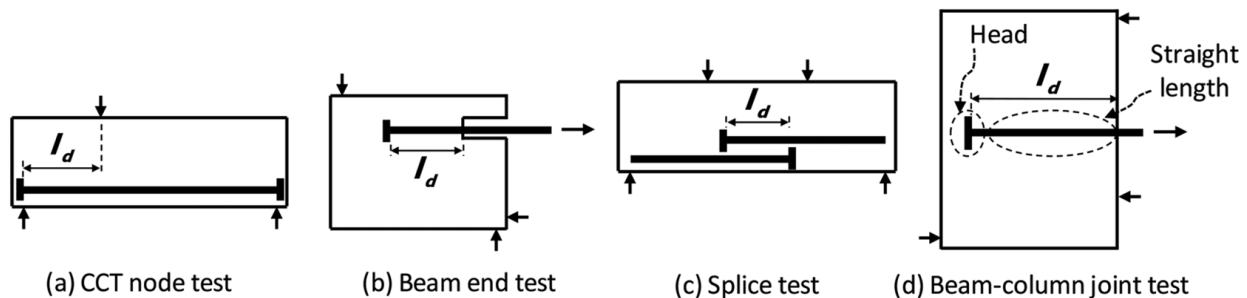
Fig. 1 Test methods for headed bar bond strength

Recently, machine learning has been widely used in civil engineering. With the advanced computer intelligence, it is possible to transform input data into a more abstract and composite representation. Although several ANN models were developed for predicting bond performance of straight or hooked bars (Golafshani et al., 2012; Hwang et al., 2019; Makni et al., 2014; Mashrei et al., 2013), no attempt has been made on development of ANN model aimed for headed bars, primarily due to lack of test results on headed bars.

In the present study, to improve design reliability, an artificial neural network model (ANN, a machine learning algorithm) is presented using existing experimental studies for beam-column joint test (total 297 specimens). Although some of the test parameters are out of limitation in design codes, all test results were included for the ANN to extend design application range considering the present-day construction materials and practices.

2. EXISTING DESIGN METHODS

ACI 318-19 (ACI Committee 318, 2019) permits the use of headed bars satisfying Class HA heads specified in ASTM A970 as follows:

1. The bearing face of a headed bar should be flat face and perpendicular to the longitudinal axis of the reinforcing bars.
2. The minimum net head bearing area, which is the gross area of the head minus the cross-sectional area of the reinforcing bar, should be at least four times the nominal cross-sectional area of the reinforcing bar (i.e., $A_{nh} \geq 4A_b$).
3. The length and diameter of interruptions for connection between the reinforcing bar and bearing face should not be greater than $2d_b$ and $1.5d_b$, respectively.
4. The bearing force of the head should be greater than the minimum specified tensile strength of the reinforcing bar.

In ACI 318-19 (ACI Committee 318, 2019), Model Code 2010 (International Federation for Structural Concrete (fib), 2013), Thompson et al., (Thompson et al., 2006) and Shao et al., (Shao et al., 2016) the development length l_d of headed bars is defined as a function of reinforcing bar diameter, reinforcing bar yield strength, and concrete compressive strength. Additionally, the effects of concrete cover, bar spacing, transverse reinforcement, and head bearing force are considered (Fig. 2).

In ACI 318-19 (ACI Committee 318, 2019), the development length of a headed bar is defined as follows.

$$l_d = \frac{0.19 f_y d_b \psi_e}{\sqrt{f_c'}} \geq 8d_b \quad \text{and 152.4 mm} \tag{1}$$

where f_y is yield strength of the headed bar; d_b is reinforcing bar diameter; f_c' is concrete compressive strength; and ψ_e is coefficient of epoxy-coated bars (= 1.0 to 1.2). Unlike the development length of hooked bars, the effects of concrete cover, confining bar, and concrete type on the development length are not considered. Instead, the use of **Eq. (1)** is limited to the following design conditions: f_y less than 414 MPa, d_b less than 35.8 mm, normal-weight concrete, clear cover thickness of at least $2d_b$, and clear spacing between reinforcing bars of at least $4d_b$.

3. ARTIFICIAL NEURAL NETWORKS

3.1 Model composition

Figure 2(a) shows the artificial neural networks, which consists of an input layer, a hidden layer, and an output layer. For simplicity, only one hidden layer was shown in **Figure 2(a)**, but multiple numbers of hidden layer were actually used to solve complicated nonlinearity between parameters. The input layer receives the values of the selected input variables, and each node of the input layer is connected to nodes of the hidden layer. As a constant value, a bias (b) was included in the input layer (also in the hidden layer). The values entering a hidden node were determined after multiplying the input and bias by weights ($w_{i,j}$) as follows.

$$z_j^{(1)} = \sum_{i=1}^{n+1} w_{i,j}^{(1)} x_i \tag{2}$$

where $z_j^{(1)}$ = input value at the *j*-th node of the hidden layer; $w_{i,j}^{(1)}$ = weight between the *i*-th input node and the *j*-th hidden node; *i* = location of an input node (1 to *n* + 1 including a bias node); *j* = location of a hidden node (1 to m); *n* = total number of the selected input variables; and *m* = total number of hidden nodes except a bias node. It is noted that the value of each input node was normalized to be between 0 and 1, $w_{n+1,j}^{(1)} = b_j^{(1)}$ and $w_{n+1} = 1$ to consider the bias in the input layer, and the values of weight ($w_{i,j}^{(1)}$) and bias ($b_j^{(1)}$) were randomly initialized to be between 0 and 1 at the initial step and then updated by training.

The Relu function was used for the activation function in the hidden layer to transform $z_j^{(1)}$ into $y_j^{(1)}$.

$$y_j^{(1)} = f_1\left(z_j^{(1)}\right) = max\left(z_j^{(1)}, 0\right) \tag{3}$$

where $y_j^{(1)}$ = output value at the *j*-th hidden node, which is between 0 and 1. The output values of hidden modes and a bias (*b*) are concentrated on a node of the output layer.

$$z^{(2)} = \sum_{j=1}^{m+1} w_{j,i}^{(2)} y_j^{(1)} \tag{4}$$

where $z^{(2)}$ = input value at the node of the output layer; and $w_{j,i}^{(2)}$ weight between the *j*-th hidden node and the output node. It is noted that = $w_{m+1,1}^{(2)} = b_1^{(2)}$ to consider the bias in the hidden layer, and the values of weight ($w_{j,i}^{(2)}$) and bias ($b_1^{(2)}$) were randomly initialized to be between 0 and 1 at the initial step and then updated by training.

In the output layer, a linear activation function was used to determine the final output value (*y*).

$$y_j^{(1)} = f_2\left(z^{(2)}\right) = z^{(2)} \tag{5}$$

(a) Artificial neural networks with a hidden layer

(b) Back propagation in artificial neural networks with a hidden layer
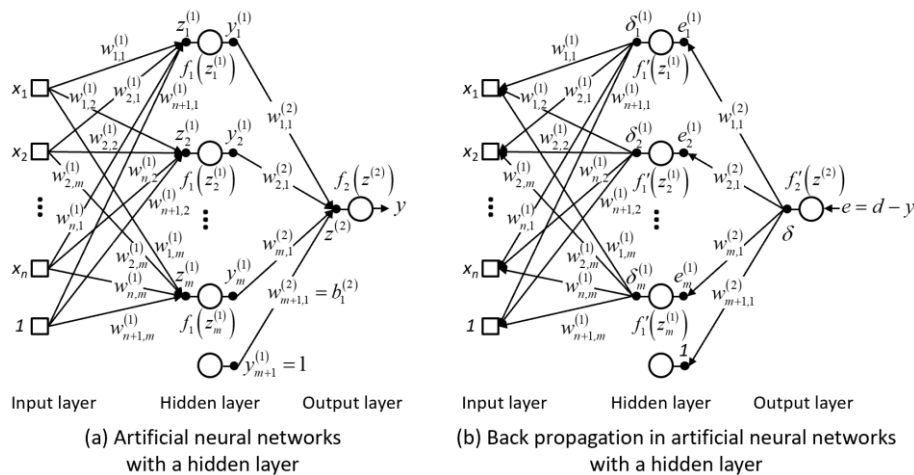
Fig. 2 Artificial neural networks for headed bars in this study

3.2 Back propagation

Figure 2(b) shows the back propagation for updating the weight and bias in each layer. On the basis of the back propagation algorithm (Rumelhart et al., 1986), the weight between the hidden and output layers can be updated by the weight increment $w_{j,1}^{(2)}$, which is calculated from the output value $y_j^{(1)}$ at the *j*-th hidden node and the difference between the actual output (or final output value, *y*) and expected output (or normalized target value, *d*) for learning. It is noted that *j* = 1 to m+1 are used to update $w_{m+1,1}^{(2)}$ for the bias.

$$e = d - y \tag{6a}$$

$$\delta = f_2'\left(z^{(2)}\right)e = e \tag{6b}$$

$$\Delta w_{j,i}^{(2)} = \alpha\delta y_j^{(1)} = \alpha\delta(d - y) \tag{6c}$$

$$\left[m_{j,1}^{(2)}\right]_k = \left[\Delta w_{j,1}^{(2)}\right]_k + \beta\left[\Delta m_{j,1}^{(2)}\right]_{k-1} \tag{6d}$$

$$\left[w_{j,1}^{(2)}\right]_{k+1} = \left[w_{j,1}^{(2)}\right]_k + \left[m_{j,1}^{(2)}\right]_k \tag{6e}$$

where *e* = error; *α* = training ratio (0 to 1); *β* = coefficient related to momentum training ratio (0 to 1); *k* = number of training data; and $\left[m_{j,1}^{(2)}\right]_0$ = initial momentum to improve the stability of learning (set as 0). In the same manner, the weight $w_{i,j}^{(1)}$ between the input and hidden layers can be updated as follows.

$$e_j^{(1)} = w_{j,1}^{(2)} \times \delta = w_{j,1}^{(2)}(d - y) \tag{7a}$$

$$\delta_j^{(1)} = f_1'\left(z_j^{(1)}\right) \times e_j^{(1)} = \left(1 + f_1'\left(z_j^{(1)}\right)\right)\left(1 - f_1'\left(z_j^{(1)}\right)\right)e_j^{(1)} \tag{7b}$$

$$\Delta w_{j,i}^{(1)} = \alpha\delta_j^{(1)}x_i \tag{7c}$$

$$\left[m_{j,1}^{(1)}\right]_k = \left[\Delta w_{i,j}^{(1)}\right]_k + \beta\left[m_{i,j}^{(1)}\right]_{k-1} \tag{7d}$$

$$\left[w_{i,j}^{(1)}\right]_{k+1} = \left[w_{i,j}^{(1)}\right]_k + \left[m_{i,j}^{(1)}\right]_k \tag{7e}$$

where $\left[m_{j,1}^{(1)} \right]_0$ = initial momentum to improve the stability of learning (set as 0); and $j = 1$ to m are used to update $w_{i,j}^{(1)}$.

All weights in **Eqs. (2)–(7)** were updated by using the training data. The calculations should be iterated until the accuracy converges into a target level or cannot be improved above a certain level. Thereafter, the ANN with the fixed values of weight can be used for prediction through **Eqs. (2)–(5)**. It is noted that since **Eq. (5)** estimates the normalized y between 0 and 1, inverse normalization is necessary based on the normalized d for final prediction. Detailed descriptions are given in the next section.

3.3 Application

Design equations have limitations on their application because of lack of adequate experimental data. However, to extend design application range considering present-day construction materials and practices, the ANN was applied to 297 existing experimental studies for beam-column joint test, some of whose parameters are beyond the limitations of current design codes. Because current design provisions were established based on the bar tensile stress in a given splice length of the splice tests, the bar tensile stress was predicted using the ANN. Then, the ANN was trained by comparing the predicted and measured bar tensile stresses. The following variables were used in the input layer (9 input nodes including a bias node of 1) on the basis of existing design equations. In the ANN, the development length of $l_d = l_s$ was used.

$$\left[x_i \right]_{i=1 \sim n+1} = \begin{bmatrix} l_d & d_b & f_c' & f_y & \dfrac{A_{tr}}{n_s s_t d_b} & \dfrac{c_b}{d_b} & \dfrac{c_{so}}{d_b} & \dfrac{c_{so}}{d_b} & 1 \end{bmatrix} \tag{8}$$

For data learning, the variables were normalized as follows, and put into **Eq. (8)**.

$$x_i = \frac{x_i - x_{i,min}}{x_{i,max} - x_{i,min}} \tag{9}$$

where $x_{i,min}$ and $x_{i,max}$ = minimum and maximum values of a variable at the i-th input node, respectively. Using **Eq. (9)**, the normalized target value (d) can be calculated from the test results f_t. After data learning, the predicted tensile stress f_p of bar splices was calculated from the final output value y.

$$f_p = y \left(f_{t,max} - f_{t,min} \right) + f_{t,min} \tag{10}$$

where $f_{t,min}$ and $f_{t,max}$ = minimum and maximum values of actual tensile stress of bar splices.

Of the 270 specimens, 80% (216 specimens) were used for training and validation (20%), and the remaining 20% (54 specimens) were used for verification. In the training, total 6 hidden layers were used with the number of hidden nodes reducing (i.e., $m + 1 = 10000, 5000, 2500, 1250, 625,$ and $50, \alpha$ was 0.0001 according to an error level in the both of training and verification, and $\beta = 0.1$ was used. Strain hardening of reinforcing

bars was neglected in learning according to existing design codes (ACI Committee 318, 2019; ACI Committee 408, 2003; British Standards Institution, 2003; International Federation for Structural Concrete (fib), 2013) (i.e., the maximum value of f_t was limited to the yield strength f_y of reinforcing bars). The final weight matrices $w_{i,j}^{(1)}$ and $w_{j,1}^{(2)}$ for the input and hidden layers were obtained after performing about 1000-step trainings, and these matrix-typed models for input variables can be used for practical application.

Figure 3(a) show the loss values with training number (i.e., epoch). Both losses of training data and validation data converged into a certain value as the epoch was increased. Thus, the model at 1000 epoch was considered appropriately fitted. **Figure 3(b)** compares the actual tensile stress f_t in reinforcing bars by testing and the predicted tensile stress $f_{t,pred}$ by the ANN model. The R^2 score of the model was 0.8977, and the coefficient of the variance (cov) was 0.1306, which indicates that the model generated by the ANN model can be superior to the existing model.

(a) Loss versus epoch relationships

(b) Comparison between tested tensile stress and predicted tensile stress in reinforcing bars in beam–column joint test
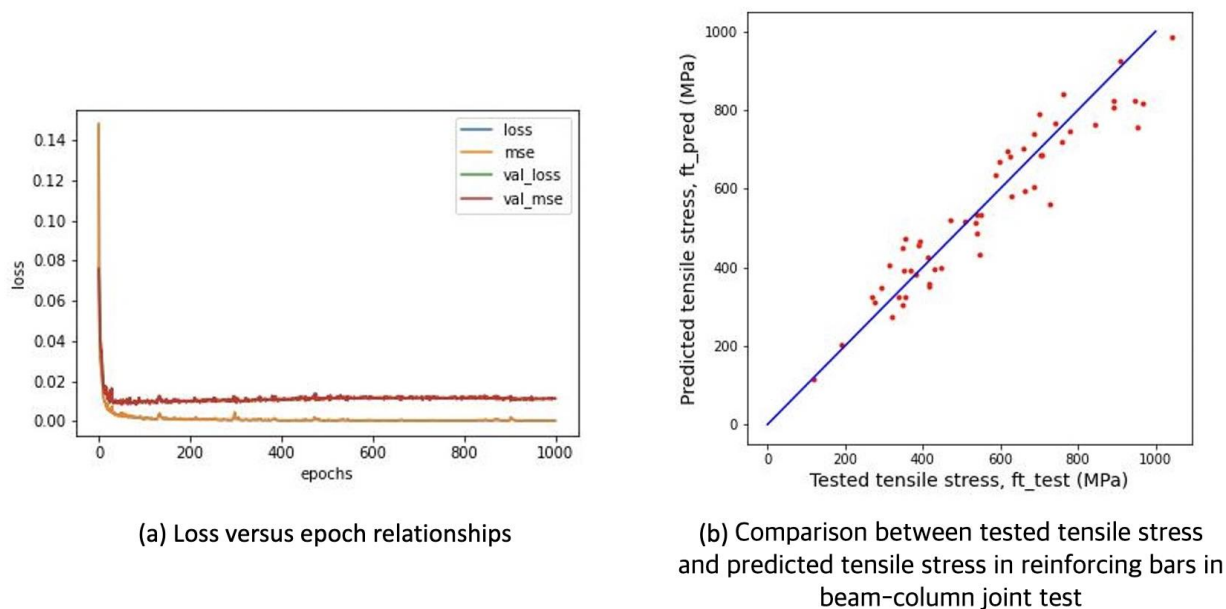
Fig. 3 Results of ANN development for headed bars using beam-column joint test

4. SUMMARY AND CONCLUSIONS

The anchorage capacity of headed bars shows large variations according to design conditions, such as diameter of reinforcing bars, location of anchorage, and the use of fiber-reinforced concrete. To use headed bars in various design conditions, the development length of headed bars needs to be accurately evaluated and a large number of test results are required to verify the effect of new design parameters. In the present study, to improve design reliability, an artificial neural network model (ANN, a machine learning algorithm) is presented using existing experimental studies for beam-column joint test (total 270 specimens).

The major findings of the ANN model for the headed bars are summarized as follow:

1. A deep leaning model was generated with important parameters of headed bars. The network consists of 6 layers and many nodes to solve the complicated relationships between the major parameters.
2. Both losses of training data and validation data converged into appropriately small values at around 1000 epoch.
3. In the relationships between the actual tensile stress f_t in reinforcing bars by testing and the predicted tensile stress $f_{t,pred}$ by the ANN model, the R^2 score of the model was 0.8977, and the coefficient of the variance (cov) was 0.1306, which indicates that the model generated by the ANN model can be superior to the existing model.
4. Parametric studies should be implemented to address the effect of each parameter.
5. For better reliability and performance of the ANN model, appropriate train-test set split method should be adopted.
6. In addition to the beam-column joint type specimens, the test results incorporating other types of headed bar test such as CCT node test, Beam-end test, or splice test as shown in **Fig. 1** are needed to develop integrated predictive ANN model for headed bars.

ACKNOWLEDGEMENT

REFERENCES

ACI Committee 318. (2019). Building Code Requirements for Structural Concrete (ACI 318-19): An ACI Standard: Commentary on Building Code Requirements for Structural Concrete (ACI 318R-19). In (pp. 623). Farmington Hills, MI: American Concrete Institute.

ACI Committee 408. (2003). Bond and Development of Straight Reinforcing Bars in Tension (ACI 408R-03). In (pp. 49). MI: American Concrete Institute, Farmington Hills.

British Standards Institution. (2003). Eurocode 8: Design of Structures for Earthquake Resistance. In (Vol. Part 1: General Rules, Seismic Action and Rules for Buildings, pp. 229). Bruxelles : CEN: European Committee for Standardization.

Golafshani, E. M., Rahai, A., Sebt, M. H., & Akbarpour, H. (2012). Prediction of bond strength of spliced steel bars in concrete using artificial neural network and fuzzy logic. *Construction and Building Materials, 36*, 411-418.

Hwang, H.-J., Park, H.-G., & Yi, W.-J. (2019). Development length of headed bar based on nonuniform bond stress distribution. *ACI Structural Journal, 116*(2), 29-23.

International Federation for Structural Concrete (fib). (2013). fib Model Code for Concrete Structures 2010. In (pp. 402). Berlin, Germany: Wilhelm Ernst & Sohn.

Makni, M., Daoud, A., Karray, M. A., & Lorrain, M. (2014). Artificial neural network for the prediction of the steel–concrete bond behaviour. *European journal of environmental and civil engineering, 18*(8), 862-881.

Mashrei, M. A., Seracino, R., & Rahman, M. (2013). Application of artificial neural networks to predict the bond strength of FRP-to-concrete joints. *Construction and Building Materials, 40*, 812-821.

Rumelhart, D. E., Hinton, G. E., & Williams, R. J. (1986). Learning representations by back-propagating errors. *nature, 323*(6088), 533-536.

Shao, Y., Darwin, D., O'Reilly, M., Lequesne, R. D., Ghimire, K. P., & Hano, M. (2016). *Anchorage of conventional and high-strength headed reinforcing bars*. Retrieved from

Thompson, M. K., Jirsa, J. O., & Breen, J. E. (2006). Behavior and capacity of headed reinforcement. *ACI Materials Journal, 103*(4), 522.